MOLECULAR PHYSICS, 1993, VOL. 79, NO. 4, 709–720

On one-dimensional fluids of anisotropic molecules near a hard wall

By F. S. FERRERO, B. MARTÍNEZ-HAYA, J. M. PASTOR, J. A. CUESTA and C. F. TEJERO

Facultad de Ciencias Físicas, Universidad Complutense de Madrid, 28040-Madrid, Spain

(*Received 25 September 1992; accepted 20 October 1992*)

A separable one-dimensional model of anisotropic hard molecules recently introduced in the literature is worked out to compute the radial density profiles and the angular distributions in the vicinity of a hard wall. Its results are tested against Monte Carlo simulations performed on a system of aligned hard ellipses confined in a segment. We find that the model provides a good description of such a system whenever the angular mobility of the particles is small enough. Accordingly, we find that the density profiles are better described for high pressures, and the angular distributions when they are close to the wall. Nevertheless, the distribution functions in the bulk have the same functional shape but for a smaller eccentricity. Such effective eccentricities follow a power law extremely well when compared with the true ones.

1. Introduction

The statistical mechanical description of the equilibrium properties of one-dimensional (1D) fluids with nearest neighbour interactions has attracted the interest of physicists since the pioneering works of Rayleigh [1] and Tonks [2] concerning the equation of state of a 1D system of hard rods. Salsburg *et al.* [3] further extended these studies by determining the distribution functions of the homogeneous hard rod fluid, and the direct correlation function was obtained in a later work by Percus [4]. In recent years, attention has been shifted to the study of inhomogeneous fluids. Semi-infinite systems, fluids confined by hard walls, and fluids in an arbitrary external field have been investigated in detail. The main interest of these model systems is to provide approximations for a microscopic theory of real fluids in contact with walls or adsorbed at solid substrates. Functional methods were first developed by Percus [5], who obtained the one-body density and the direct correlation function of a fluid with sticky-core interactions near a hard wall. Fluids confined on a line of finite length have been analysed by Leff and Coopersmith [6] and Robledo and Rowlinson [7]. Absorption of 1D hard rods in a hard wall has been obtained with computer simulation by Finn and Monson [8]. 1D mixtures of hard rods [9] and square-well fluids [10] have recently been considered for describing selective adsorption. Also polymerization has been studied with 1D models of associating hard rods in an external field [11].

For 1D fluids with anisotropic hard core interactions very little work has been done. The orientational properties of some of these models have recently been investigated by Lebowitz *et al.* [12]. In the case where the molecules are assumed to have a single rotational degree of freedom (say, ellipses in a plane with their centres of mass restricted to lie on the x axis) the hard core diameter (contact

0026-8976/93 $10.00

distance) depends quite generally on the orientations of two neighbouring molecules. Nevertheless, a separable model can be introduced in which this diameter is written as a sum of two terms, each one containing the orientation of a molecule. The thermodynamics [12] and structure [13] of this model can be determined exactly in the bulk. Although the separable model reproduces the exact results for hard anisotropic bodies in the high pressure limit [12, 13], very little is known about how it is related to these systems at finite pressures.

In this paper, we extend the study of the separable model to include the calculation of the radial and angular distributions in the vicinity of a hard wall. We also perform a Monte Carlo (MC) simulation for the hard ellipse system to test the results of the theory. We find surprisingly good agreement for such a simple model, so that it can be considered as a first approach to the study of liquid crystal phases in contact with solid surfaces.

2. Model

As a representative model of a 1D system of N anisotropic hard convex bodies, let us consider freely rotating ellipses in a plane with their centres of mass restricted to move along a segment of length L. These ellipses interact via a nearest neighbours hard core potential, which we denote by

$$\phi(|x-x'|;\varphi,\varphi') = \begin{cases} 0 & |x-x'| > \sigma(\varphi,\varphi') \\ \infty & |x-x'| < \sigma(\varphi,\varphi') \end{cases}, \tag{1}$$

where $\sigma(\varphi,\varphi')$ is the contact distance between two neighbouring ellipses with orientations φ and φ'. We can write down the expression for the partition function of such a system as

$$Z_N(\beta,L) = \mathrm{Tr}\,\exp\left\{-\beta\sum_{j=0}^{N}\phi(|x_j-x_{j+1}|;\varphi_j,\varphi_{j+1})\right\}, \tag{2}$$

with $\beta = 1/k_B T$ the inverse of the temperature in units of the Boltzmann's constant, and the trace defined as

$$\mathrm{Tr} \equiv \prod_{j=1}^{N}\int_{-\pi}^{\pi}\frac{\mathrm{d}\varphi_j}{2\pi}\int_0^L \mathrm{d}x_j \tag{3}$$

Since we have hard walls at the extremes of the interval, the boundary conditions can be implemented as the interaction of the first and last particles with their mirror images with respect to the extremes of the segment. Thus, $x_0 = -x_1$, $\varphi_0 = -\varphi_1$, $x_{N+1} = 2L - x_N$ and $\varphi_{N+1} = -\varphi_N$.

As formulated, this problem is too general to be solved analytically, although a few exact results can be obtained from equation (2) by a transfer-matrix formalism [12]. However, it has also been pointed out that the partition function (2) can be computed if the contact distance is assumed separable, i.e.

$$\sigma(\varphi,\varphi') = \tfrac{1}{2}[\sigma(\varphi)+\sigma(\varphi')], \tag{4}$$

which for the system of hard ellipses is an approximation that is valid when the mobility of the particles is small enough. This model was tested against the exact results of [12] and was found to behave reasonably well [13]. Besides, it has the great advantage that its properties can be obtained analytically. The point is that with the

approximation (4) the partition function is similar to that of hard rods with variable lengths $\sigma(\varphi_j)$ averaged over the angles φ_j; that is,

$$Z_N(\beta, L) = \left\langle \Theta\left(L - \sum_{j=1}^{N} \sigma(\varphi_j)\right) \frac{[L - \Sigma_{k=1}^{N} \sigma(\varphi_k)]^N}{N!} \right\rangle, \tag{5}$$

where the average denotes the normalized integration over the angular variables, i.e., $\langle \cdot \rangle \equiv \Pi_{j=1}^{N} \mathrm{d}\varphi_j/2\pi$, and $\Theta(x)$ is the Heaviside step function. The result becomes simpler in the isobaric ensemble, where the isobaric partition function is obtained as

$$Q_N(\beta, P) = \int_0^\infty \mathrm{d}L \mathrm{e}^{-\beta P L} Z_N(\beta, L) = \frac{1}{\beta P} \left[\frac{I(\beta P)}{\beta P}\right]^N. \tag{6}$$

In this formula, P stands for the pressure and $I(x)$ denotes the integral

$$I(x) \equiv \int_{-\pi}^{\pi} \frac{\mathrm{d}\varphi}{2\pi} \mathrm{e}^{-x\sigma(\varphi)}. \tag{7}$$

3. Density profiles near a hard wall

The ability of this model to be worked out analytically will be used in this section to study the radial and angular distribution profiles of the system of hard ellipses near a wall. The definition of the 1-body distribution function in the canonical ensemble is

$$\rho_L(x, \varphi) \equiv \sum_{k=1}^{N} \langle \delta(x - x_k) \delta(\varphi - \varphi_k) \rangle_{\mathrm{can}}. \tag{8}$$

In our separable model this distribution has the form

$$\rho_L(x, \varphi) = \frac{1}{Z_N(\beta, L)} \sum_{k=1}^{N} Z_{k-1}(\beta, x - \tfrac{1}{2}\sigma(\varphi)) Z_{N-k}(\beta, L - x - \tfrac{1}{2}\sigma(\varphi)). \tag{9}$$

As in the previous section, let us introduce the distribution function in the isobaric ensemble:

$$\begin{aligned} \rho_P(x, \varphi) &\equiv \sum_{k=1}^{N} \langle \delta(x - x_k) \delta(\varphi - \varphi_k) \rangle_{\mathrm{iso}} \\ &= \frac{1}{Q_N(\beta, P)} \int_0^\infty \mathrm{d}L \mathrm{e}^{-\beta P L} Z_N(\beta, L) \rho_L(x, \varphi). \end{aligned} \tag{10}$$

The integration can be performed easily by using equation (5). The result, which for convenience will be expressed in terms of the variable $y = x - \sigma(\varphi)/2$, is

$$\rho_P(y, \varphi) = \mathrm{e}^{-\beta P(y + \sigma(\varphi))} \sum_{k=1}^{N} Z_{k-1}(\beta, y) \left[\frac{\beta P}{I(\beta P)}\right]^k. \tag{11}$$

To evaluate the latter expression it is necessary to Laplace transform in the y variable. Thus, the transformed profile turns out to be, in the thermodynamic limit,

$$\begin{aligned} \tilde{\rho}_P(s, \varphi) &\equiv \int_0^\infty \mathrm{d}y \mathrm{e}^{-sy} \rho_P(y, \varphi) \\ &= h(\varphi) \frac{\beta P}{s + \beta P(1 - \langle \mathrm{e}^{-s\sigma(\varphi)} \rangle_h)}, \end{aligned} \tag{12}$$

where

$$h(\varphi) \equiv \frac{e^{-\beta P \sigma(\varphi)}}{I(\beta P)}, \tag{13}$$

and $\langle \cdot \rangle_h \equiv \int_{-\pi}^{\pi} \cdot \, h(\varphi) \, d\varphi / 2\pi$.

Equation (12) gives us information on the behaviour of $\rho_P(y, \varphi)$ in the limits $y \to \infty$ (bulk) and $y \to 0$ (closest distance to the wall) through the Tauberian theorem [14]. This theorem states that if $F(t)$ is a non-decreasing function and if the integral defined by

$$f(s) = \int_0^{\infty} e^{-st} \, dF(t) \tag{14}$$

(provided it converges for Re $s > 0$) behaves, in the limit $s \to 0$ ($s \to \infty$), as

$$f(s) \sim s^{-\gamma} L(1/s), \tag{15}$$

with $\gamma > 0$, then, in the limit $t \to \infty$ ($t \to 0$) $F(t)$ behaves as

$$F(t) \sim \frac{t^{\gamma} L(t)}{\Gamma(\gamma + 1)}. \tag{16}$$

Direct application of the theorem to equation (12) yields

$$\lim_{y \to \infty} \rho_P(y, \varphi) = \frac{\beta P}{1 + \beta P \langle \sigma(\varphi) \rangle_h} h(\varphi), \tag{17}$$

$$\lim_{y \to 0} \rho_P(y, \varphi) = \beta P h(\varphi). \tag{18}$$

Note that, for isotropic bodies ($h(\varphi) \equiv 1$), equation (18) implies that the well known sum rule for hard walls [15] is exactly verified.

Transforming $\tilde{\rho}_P(s, \varphi)$ back to obtain the density profile is a difficult task that can be achieved only numerically. For this purpose it is easier to work with the Fourier transform instead of the Laplace transform. The former can be obtained from the latter through the simple relation

$$\hat{\rho}_P(q, \varphi) = \tilde{\rho}_P(iq, \varphi) + \tilde{\rho}_P(-iq, \varphi). \tag{19}$$

This equation holds only for Laplace transforms with no singularities, something that equation (12) violates (it is singular for $s = 0$). The reason for this divergence is that $\rho_P(y, \varphi)$ is non-integrable, since it tends to a non-zero value for $y \to \infty$. It is easy, however, to circumvent this difficulty by applying equation (19) to the adsorption function $\rho_P^{abs}(y, \varphi) \equiv \rho_P(y, \varphi) - \rho_P(\infty, \varphi)$ instead. This yields

$$\hat{\rho}_P^{abs}(q, \varphi) = \frac{2[1 - \langle \cos(q\sigma(\varphi)) \rangle_h]}{[1 - \langle \cos(q\sigma(\varphi)) \rangle_h]^2 + \left[\frac{q}{\beta P} + \langle \sin(q\sigma(\varphi)) \rangle_h \right]^2} h(\varphi), \tag{20}$$

where the averages can be expressed in terms of $I(x)$ (equation (7)) as

$$\langle \cos(q\sigma(\varphi)) \rangle_h = \frac{I(\beta P - iq) + I(\beta P + iq)}{2I(\beta P)}, \tag{21}$$

$$\langle \sin(q\sigma(\varphi)) \rangle_h = \frac{I(\beta P - iq) - I(\beta P + iq)}{2iI(\beta P)}. \tag{22}$$

Now the computation of the adsorption function is carried out by numerically transforming back equation (20), with the choice of $\sigma(\varphi)$ suggested in [12] and [13], i.e. $\sigma(\varphi) = \sigma[(\kappa + 1) - (\kappa - 1)\cos(2\varphi)]/2$, where σ is the minor diameter of the ellipse and κ is the ratio of the major diameter to σ. This particular form allows us to write $I(x) = \exp[-x(\kappa + 1)\sigma/2] I_0(x(\kappa - 1)\sigma/2)$, with $I_0(x)$ the modified Bessel function of zeroth order [16] and, consequently,

$$h(\varphi) = \frac{e^{-\gamma \cos(2\varphi)}}{I_0(\gamma)}, \tag{23}$$

with $\gamma \equiv \beta P \sigma(\kappa - 1)/2$.

4. Monte Carlo simulation

To test our analytical findings we have performed MC simulations on the hard ellipse system in a segment bounded by hard walls. Basically, we have followed the method worked out in [8] for hard rods. The simulations have been carried out in the isothermal–isobaric (T, P constant) ensemble [17]. Acceptable configurations are those for which there is no overlap between the ellipses.

A MC trial consists of moving simultaneously both the position x_i and the orientation φ_i of the ith particle. Position and orientation are changed by adding random numbers Δ_x and Δ_φ, uniformly chosen within the intervals $(-\Delta, \Delta)$ and $(-\Delta', \Delta')$. The movement is rejected if, after the change, the ellipse overlaps any of its nearest neighbours. Testing the overlap is done via Vieillard-Baron's criterion [18]. We have chosen Δ and Δ' such that the acceptance ratio is around 20–30%.

After attempting to move all particles once, a change of length trial is performed. The change is done by multiplying the current length L of the interval by a factor $\exp(\xi_L)$, where ξ_L is a random number uniformly chosen in the interval $(-\xi, \xi)$. The movement is rejected if an overlap occurs and accepted with probability

$$r \equiv \min\{1, \exp[(N + 1)\xi_L - \beta P(\exp(\xi_L) - 1)L]\} \tag{24}$$

otherwise. With this procedure we actually sample $\ln L$ instead of L itself. The reason for doing this is that in this way the domain of the generated random chain coincides with the range of acceptable values of $L (L > 0)$, thus improving the efficiency of the sampling [17, 19]. Again, ξ is chosen so as to get a length-change acceptance ratio of about 20–30%.

Table 1. Data for the packing fraction $\eta \equiv \rho\sigma$ obtained by MC simulation of the hard ellipse system compared with the theoretical (T) results of the separable model, for different aspect ratios (κ) and reduced pressures ($\beta P\sigma$). Values in parentheses are affected by statistical error. Notice the weak κ-dependence of the values.

	$\kappa = 2$		$\kappa = 4$		$\kappa = 6$	
$\beta P\sigma$	MC	T	MC	T	MC	T
0·5	0·29(4)	0·291	0·25(6)	0·252	0·23(8)	0·239
1·0	0·42(5)	0·421	0·38(3)	0·384	0·37(6)	0·387
2·0	0·57(0)	0·563	0·55(4)	0·560	0·55(7)	0·566
4·0	0·71(8)	0·714	0·72(5)	0·724	0·72(3)	0·725

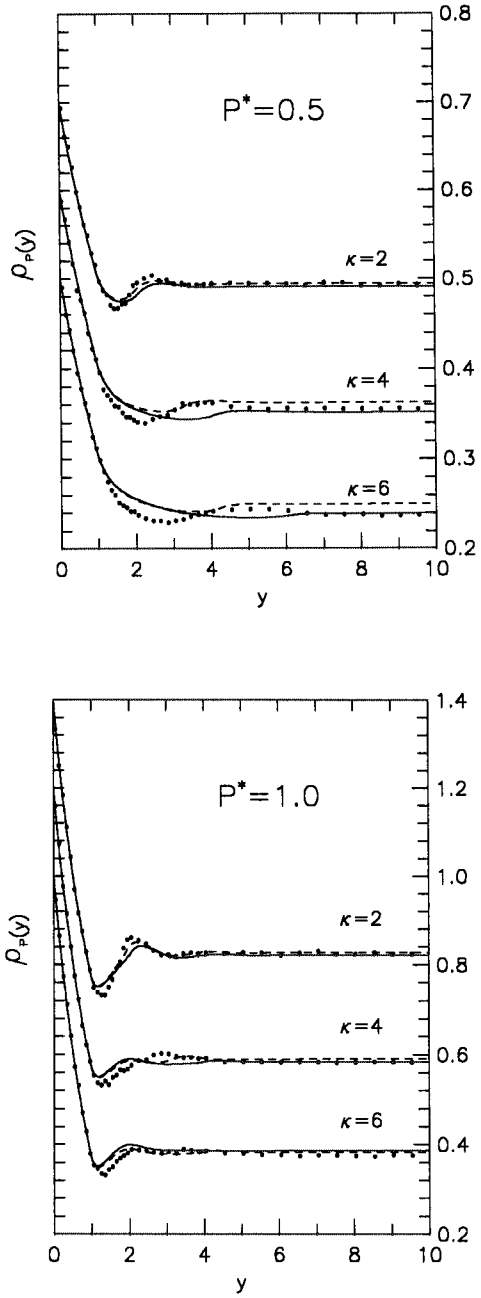

Figure 1. Radial density profiles at constant pressure $\rho_P(y) \equiv \langle \rho_P(y, \varphi) \rangle_\varphi$ as a function of y, the distance to the centre of mass of the closest particle to the wall, for different reduced pressures ($P^* \equiv \beta P \sigma$) and aspect ratios ($\kappa$). Dots are the MC results for the hard ellipse system, and solid lines are the theoretical results of the separable model. Dashed lines are the theoretical results for the effective κ obtained from the fit of equation (23) to the bulk angular distribution function (see text and figures 2 and 3). For the sake of clarity the curves are shifted upwards by 0·1 ($P^* = 0{\cdot}5$), 0·2 ($P^* = 1{\cdot}0$), 0·3 ($P^* = 2{\cdot}0$) and 1 ($P^* = 4{\cdot}0$) units with respect to the previous one.

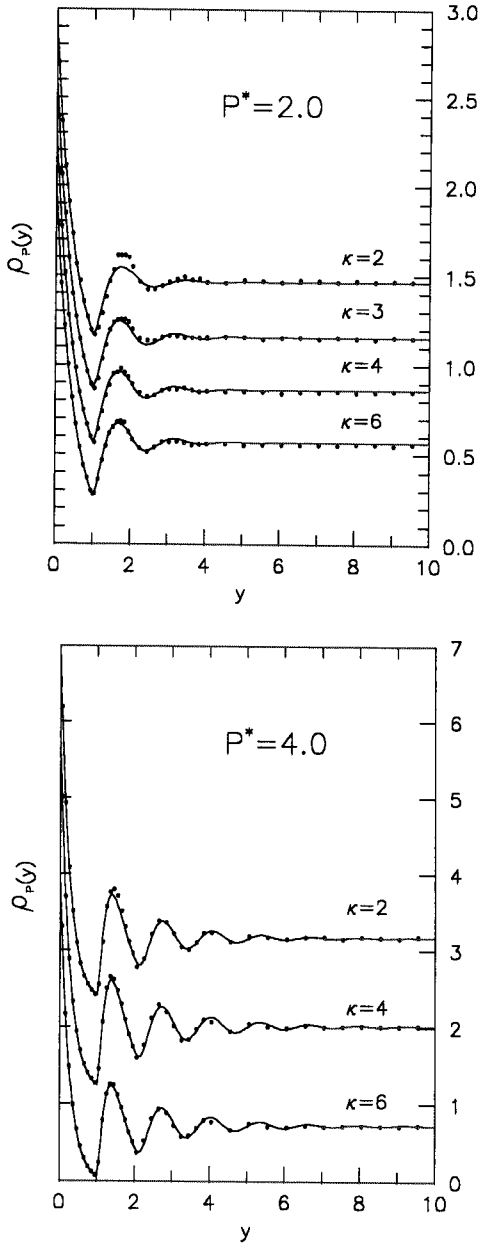

Figure 1. Continued.

As in [8] we have kept one wall fixed and performed the length changes by moving the other wall. This method reduces the number of particles needed, as it directly provides an asymmetric density profile. Besides, no strong system size dependence is expected in a 1D system. Thus, we have found, as in [8], that ten particles are sufficient to reproduce the density profile near the wall in the whole range of interest. Pressures have been chosen in a wide interval between representative values of the 'high' ($\beta P\sigma = 4$) and 'low' ($\beta P\sigma = 0{\cdot}5$) pressure limits. The system

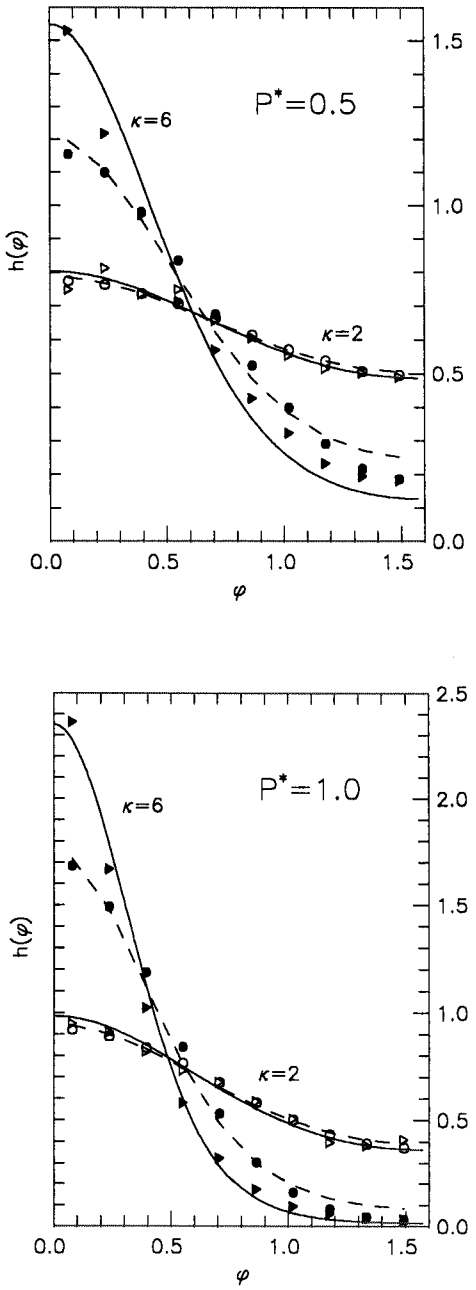

Figure 2. Angular distributions $h(\varphi) \equiv \langle \rho_P(y, \varphi) \rangle_y / \rho$ as a function of the molecular orientation φ for different reduced pressures ($P^* \equiv \beta P \sigma$) and aspect ratios ($\kappa$). The MC results at the contact with the wall and in the bulk are represented by triangles and circles, respectively. Solid lines are the angular distributions obtained from the separable model. Such curves are always closer to the MC angular distributions near the wall. Dashed lines represent the angular distributions of the model but computed for κ_{eff}, a value obtained through a least-squares fit of equation (23) to the MC data in the bulk.

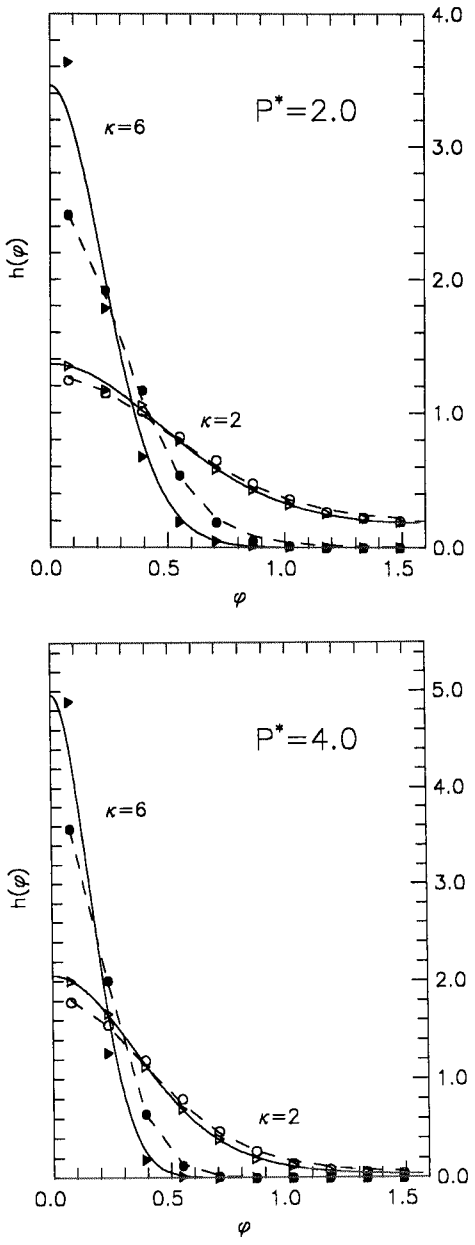

Figure 2. Continued.

has been given 10^3 MC steps (N MC trials plus an attempt of changing the box length) for equilibration, before actually computing averages along $0{\cdot}5-4 \times 10^6$ steps, the lowest (highest) number corresponding to the highest (lowest) pressure.

5. Results

The model can be tested against the simulation results at three levels: the equation of state, the radial density profiles, and the angular distributions.

The equation of state can be obtained from equation (17) by averaging over the angle φ. This yields [13]

$$\frac{1}{\rho} = \frac{1}{\beta P} + \langle \sigma(\varphi) \rangle_h, \tag{25}$$

ρ being the average density. A few values of the packing fraction ($\eta \equiv \sigma\rho$) are listed in table 1 for different values of κ and $\beta P\sigma$, together with the results obtained from the simulations. The agreement is good in all cases, in spite of the simplicity of the model. This result is not very surprising since the equation of state does not depend strongly on the details of the interaction (note that values corresponding to different κ are nevertheless very similar).

A far more crucial test is provided by comparing the radial density profiles (obtained by averaging $\rho_P(y, \varphi)$ over φ), because the structure near the wall is a direct consequence of the shape of the interaction. This comparison is made in figure 1. At first sight, the main conclusion that can be drawn from the pictures is that the larger the pressure, the better the model reproduces the profile. The reason for this is simple if one accepts that the model is more accurate when the angular mobility of the particles is small, which is precisely what happens for large pressure. On the other hand, for a given pressure the model becomes exact in the hard disk limit ($\kappa = 1$), but agreement with the simulations should also improve for $\kappa \to \infty$, because again the angular oscillations of highly elongated particles are strongly restricted. It is therefore expected that disagreement should be greatest at an intermediate value of κ. In view of the figures, such a value lies above $\kappa = 6$ for $\beta P\sigma = 0{\cdot}5$, around $\kappa = 4$ for $\beta P\sigma = 1$, and below $\kappa = 2$ for $\beta P\sigma = 2$ and 4 (note that in all these cases the maximum disagreement seems to be reached for $\gamma \approx 1$). On the whole, the model can be considered to provide a reasonably good description of the hard ellipse system in a segment for pressures above $\beta P\sigma = 1$, a regime that, according to table 1, corresponds to packing fractions higher than 0·4.

The last comparison we have performed concerns the angular distribution. An important difference between the model and the simulated system arises: while $\rho_P(y, \varphi)$ factorizes the radial and angular variables in the theoretical model, thus yielding the same angular distribution all along the segment, in the real hard ellipse system such a factorization does not take place, and so the angular distribution depends on the distance from the wall. In figure 2 the comparison is made, for different values of κ and $\beta P\sigma$, between the angular distribution (23) and that of the hard ellipse system taken at two important locations: in the bulk and at the contact with the wall. In all cases, we can see that the agreement is reasonably good for the distribution at the wall whereas it is always poor for the distribution in the bulk. The reason for this lies again in the smaller angular mobility of the particles near the wall. So far as the distribution in the bulk is concerned, we have checked the shape of the curves by fitting function (23) to the simulation data, leaving κ as a least-squares determined parameter. In this way, we obtain a curve that approaches the simulation results with a similar accuracy as the original one does with the distribution at the wall (see figure 2). The effective values of κ (κ_{eff}) so obtained show some interesting features: first of all, they are always smaller than the corresponding values of κ, thus accounting for the larger angular mobility of the particles in the bulk; second, κ_{eff} manifests a very weak dependence on the pressure; and, finally, the values obtained for κ_{eff} follow the power law extremely well

$$\kappa_{\text{eff}} \approx \kappa^{4/5}, \tag{26}$$

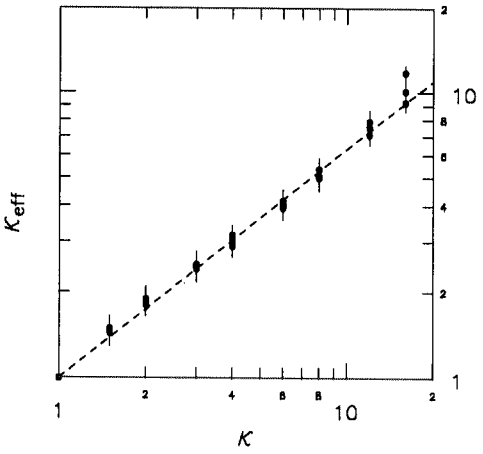

Figure 3. Effective aspect ratios κ_{eff} obtained by a least-squares fit of equation (23) to the MC data for the angular distribution function in the bulk. The dashed line is a plot of the power law $\kappa_{eff} = \kappa^{4/5}$. The different values for the same κ correspond to different pressures, and the bars give the dispersion of such values.

as shown in figure 3. On the other hand, we have plotted the radial profiles obtained with these effective eccentricities in figure 1. It can be seen that the displacement in κ affects the previous results only slightly. The largest deviations appear at the lowest pressure, where the agreement is poor anyway. Nevertheless, we can see that for $\beta P\sigma = 1$ the trend seems to be to reproduce the structure more accurately.

6. Conclusion

The test of the separable model we have worked out has shown that, in spite of its simplicity, such a model gives an overall good description of a typical 1D hard body system (in our case a hard ellipse). The model satisfies exactly the sum rule for the radial density profile near a hard wall, and yields particularly good results for the bulk or, equivalently, for the equation of state. The latter is not surprising since, as we have seen, the equation of state shows only weak dependence on the eccentricity of the molecules.

Comparison of the radial density profiles near a hard wall reveals that the model fails to describe correctly the structure at low pressures, but that the accuracy improves dramatically as the pressure increases. About the angular distributions, the model predicts the same function all along the segment—as it factorizes the radial and angular parts of the one-body distribution function—and this function reproduces rather well the profiles obtained by simulation at contact with the wall. The angular distribution of the hard ellipse system has, however, a dependence on the distance, and it broadens as it approaches the bulk. The explanation of these trends lies on the fact that the model is more realistic when the fluctuations of the particle orientations are small (something that certainly happens for high pressures and close to a hard wall).

Although the angular distribution of the model is a poor description of that of the hard ellipse system in the bulk, we have proved that the same functional shape

can be fitted well to the MC data. In this way, we obtain an effective aspect ratio (κ_{eff}), lower than the actual one (κ), for which the model describes accurately the angular distribution in the bulk. Two remarkable things about this κ_{eff} are its near independence of pressure, and the empirical power law that relates it with κ (equation (26)). Accordingly, we can also conjecture that, at a given distance y, there will be an effective aspect ratio related to κ as $\kappa_{\text{eff}}(y) = \kappa^{\alpha(y)}$, where $\alpha(0) = 1$ and $\alpha(\infty) \approx 4/5$.

We acknowledge financial support of the Dirección General de Investigación Científica y Técnica (Spain), grant no. PB88-0140.

References

[1] RAYLEIGH, LORD, 1891, *Nature*, London, **45,** 80.
[2] TONKS, L., 1936, *Phys. Rev.*, **50,** 955.
[3] SALSBURG, Z. W., KIRKWOOD, J. G., and ZWANZIG, R. W., 1953, *J. chem. Phys.*, **21,** 1098.
[4] PERCUS, J. K., 1976, *J. stat. Phys.*, **15,** 505.
[5] PERCUS, J. K., 1982, *J. stat. Phys.*, **28,** 67.
[6] LEFF, H. A., and COOPERSMITH, M. J., 1967, *J. math. Phys.*, **8,** 306.
[7] ROBLEDO, A., and ROWLINSON, J. S., 1986, *Molec. Phys.*, **58,** 711.
[8] FINN, J. E., and MONSON, P. A., 1988, *Molec. Phys.*, **65,** 1345.
[9] VANDERLICK, T. K., DAVIS, H. T., and PERCUS, J. K., 1989, *J. chem. Phys.*, **91,** 7136.
[10] MONSON, P. A., 1990, *Molec. Phys.*, **70,** 401.
[11] KIERLIK, E., and ROSINBERG, M. L., 1992, *J. stat. Phys.*, **68,** 1037.
[12] LEBOWITZ, J. L., PERCUS, J. K., and TALBOT, J., 1987, *J. stat. Phys.*, **49,** 1221.
[13] TEJERO, C. F., and CUESTA, J. A., 1990, *Physica* A, **168,** 942.
[14] KOTZ, S., and JOHNSON, N. L., 1988, *Encyclopedia of Statistical Sciences*, Vol. 9 (Wiley).
[15] EVANS, R., 1988, *Liquids at Interfaces. Les Houches, Session XLVIII*, edited by J. CHARVOLIN, J. F. JOANNY, and J. ZINN-JUSTIN (North-Holland).
[16] ABRAMOWITZ, M., and STEGUN, I. A., 1965, *Handbook of Mathematical Functions* (Dover).
[17] ALLEN, M. P., and TILDESLEY, D. J., 1989, *Computer Simulation of Liquids* (Oxford University Press).
[18] VIEILLARD-BARON, J., 1972, *J. chem. Phys.*, **56,** 4729.
[19] EPPENGA, R., and FRENKEL, D., 1984, *Molec. Phys.*, **52,** 1303.